International Journal of Mechanical Engineering and Technology (IJMET)

Volume 9, Issue 8, August 2018, pp. 296–309, Article ID: IJMET_09_07_032
Available online at http://www.iaeme.com/ijmet/issues.asp?JType=IJMET&VType=9&IType=8
ISSN Print: 0976-6340 and ISSN Online: 0976-6359

NUMERICAL ANALYSIS OF A SOLAR AIR HEATER FOR IMPROVED PERFORMANCE USING CYLINDRICAL TURBULATORS WITH RIBS

Madhwesh N

Department of Mechanical & Manufacturing Engineering,
Manipal Institute of Technology, Manipal Academy of Higher Education, Manipal, India

K. Vasudeva Karanth*

Department of Mechanical & Manufacturing Engineering,
Manipal Institute of Technology, Manipal Academy of Higher Education, Manipal, India

*Corresponding Author: kv.karanth@manipal.edu

ABSTRACT

Space heating and drying purpose for domestic, commercial and industrial applications are done these days using solar air heaters. Lot of research has been carried out to improve the performance of solar collectors using different types of turbulator design. In this study a typical cylindrical turbulator design with ribs has been analyzed for improvement in thermal performance of solar air heater. It is observed from the CFD study that there is a significant improvement in thermal performance for air heater configuration with such turbulators when compared to plain duct configuration for a wide range of mass flow rate with Reynolds number varying from 3000 to 20000. The presence of cylindrical turbulators with ribs improves the Nusselt number by about 18% for flow Reynolds number in the neighborhood of 10000 for a longitudinal turbulator pitch ratio of 1. However, at higher flow Reynolds number of 20000, the thermal performance of turbulator configuration is the highest at 12% for a pitch ratio of 0.5; This indicates that there is an optimum mass flow rate for which there is an enhanced performance related to the longitudinal pitch ratio of turbulators.

Key words: Solar air heater, pressure drop, Nusselt number, Turbulator.

Cite this Article: Madhwesh N and K. Vasudeva Karanth, Numerical Analysis of a Solar Air Heater for Improved Performance using Cylindrical Turbulators with Ribs, *International Journal of Mechanical Engineering and Technology* 9(8), 2018, pp. 296–309.
http://www.iaeme.com/IJMET/issues.asp?JType=IJMET&VType=9&IType=8

1. INTRODUCTION

Solar air heating is a renewable energy heating technology used to heat or condition the air for buildings or for process heat applications. A host of researchers have shown that the convective heat transfer capability of solar collectors can be enhanced by causing turbulence in the fluid flow and various techniques are adopted to achieve the same.

Liu et al. [1] showed that efficiency of an air heating flat plate solar collector can be increased by reducing the absorber plate temperature by providing it with extended surfaces. An experimental study showed that the absorber plate temperature decreased significantly when pin fins on the absorber plate with various configurations were provided. Persad et al. [2] developed analytical models for the performance prediction of a two-glass-cover solar air heater operated in both the single-pass and two-pass modes. It was shown that the two-pass mode of operation was superior to the single-pass mode of operation over the range of collector inlet temperatures considered. This was seen to be mainly due to the fact that, in the two-pass mode of operation, the outer glass cover was cooled by the working fluid, thereby reducing the top losses. Giovanni Tanda [3], showed that all the rib-roughened channels performed better than the reference smooth channel in the medium-low range of the investigated Reynolds number values, which are typically encountered in solar air heater applications. Karwa et.al [4] carried out thermal performance analysis of a solar air heater with downward - v discrete rib roughness on the air flow side of the absorber plate, which supplied heated air for space heating applications. The authors presented performance plots, for the purpose of utilization by a designer for calculating desired air flow rate at different ambient temperature and solar isolation values. Vasudeva et al [5] carried out a three dimensional CFD analysis to augment the performance of solar air heater. The Arc shaped turbulators were found to provide better heat transfer coefficient value compared to that of straight and V-shape turbulators. Also interestingly, Reverse arc turbulators seemed to provide better heat transfer coefficient value as compared to forward arc turbulators. Further, V-angle had no significant effect for both forward and reverse V-turbulator configurations. Abhishek et al. [6], in their review article focused on the developments that has followed in various aspects of solar air heating systems. They used several methods to enhance the thermal performance of air heaters such as; optimizing the dimensions of the air heater construction elements, use of extended surfaces with different shapes and dimensions, integrating photovoltaic elements with the heaters, etc, have been analyzed. Kabeel et al. [7] in their study, carried out the thermal performances analysis of flat, finned, and v-corrugated plate solar air heaters. It was found that the thermal efficiency of the v-corrugated solar air heater was 8–14.5% and 6–10.5% higher than that of the flat and finned plate heaters, respectively. Satyender et al. [8] studied the thermal performance of a single-pass single-glass cover solar air heater consisting of semicircular absorber plate finned with rectangular longitudinal fins. Results revealed that the use of double-glass cover and recycle operation improved the thermal performance of solar air heater. Manjunath et al. [9] studied the influence of spherical turbulence generators on thermohydraulic performance and thermal efficiency of solar flat plate air heater. The thermal efficiency was found to improve with increasing sphere diameter and reducing relative roughness pitch. Manjunath et al. [10] studied the influence of sinusoidal shaped absorber plate on enhanced heat transfer capability and related thermo-hydraulic performance of solar collector using CFD for a wide range of flow Reynolds number. The effective efficiency of the sinusoidal corrugations were found to be significant at lower flow Reynolds number conditions and in general had a narrow useful operating range of mass flow rates.

It is seen from the literature that even though there has been a lot of research carried out on the performance of air heaters with various shape and size of turbulators, the possibility of using cylindrical shaped fin turbulators with ribs is not yet explored and hence this study analyzes the possibility of using such turbulators for performance enhancement of air heaters. The study is carried out using the three dimensional numerical simulation techniques.

2. GEOMETRIC CONFIGURATION

The air heater geometry is made up of a rectangular cross section duct which has an absorber plate attached on top surface which is exposed to solar radiation. To stabilize the flow inside the absorber duct, an entrance duct and an exit duct is provided to the absorber duct at its upstream and downstream region. The dimension details of the model are as shown in figure 1.

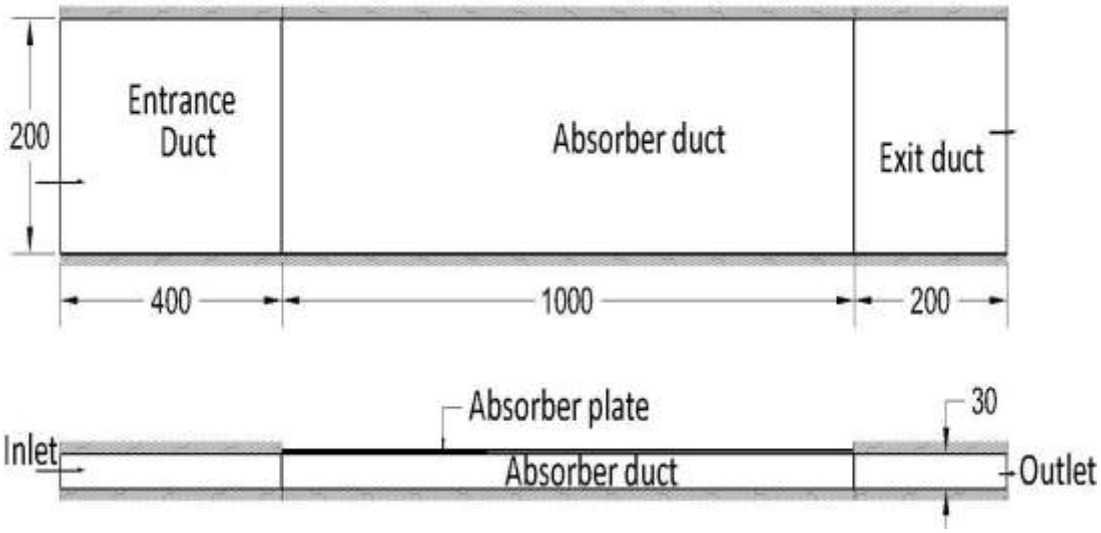

Figure 1 Schematic diagram of the air heater plain configuration

The entrance and exit duct length are adopted as per ASHRAE standards. The CFD computational domain of the solar air heater is modeled as shown in figures 2, 3 and 4. The plain configuration is made up of a smooth rectangular duct with an absorber plate of 0.5 mm thickness attached at the top surface as shown in figure 2. The configuration with turbulators is modeled as shown in figures 3 and 4 where the turbulator made up of copper material of the shape shown in figure 4a, is attached to the absorber plate from below. The turbulator core which is of diameter *d* and height 30 mm is provided with ribs of 1 mm thickness and of diameter 2d so as to enhance the turbulating action inside the absorber duct.

The turbulators are placed with a longitudinal pitch ratio r_p of 0.5, 1 and 1.5. However along the transverse direction alternatively 2 and 3 turbulators are provided with equal spacing between them. The pitch ratio r_p is taken as the ratio of the distance between the two rows of turbulator along the longitudinal direction to that of the width of the duct.

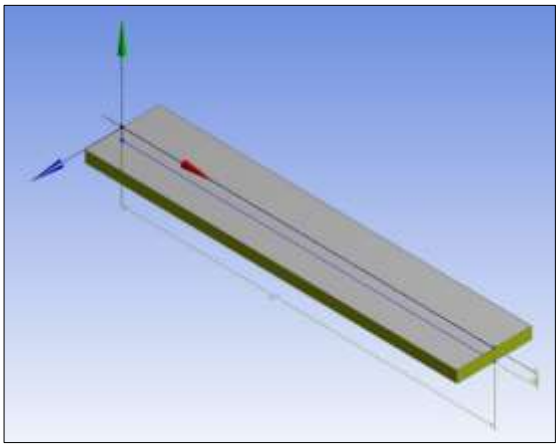

Figure 2 Plain configuration of absorber duct

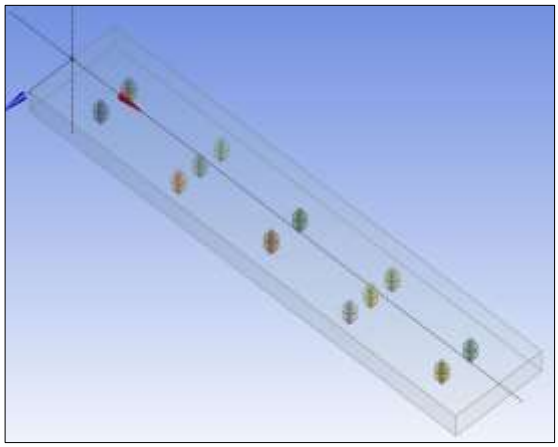

Figure 3 Turbulator configuration of absorber duct.

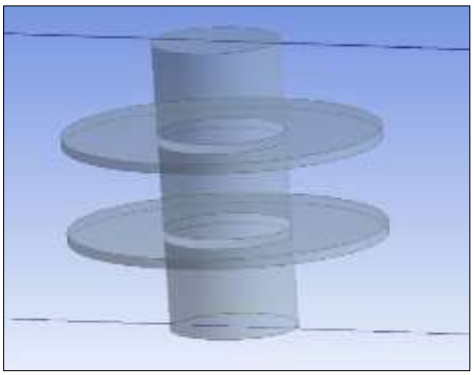

Figure 4a: Cylindrical fin turbulator with ribs

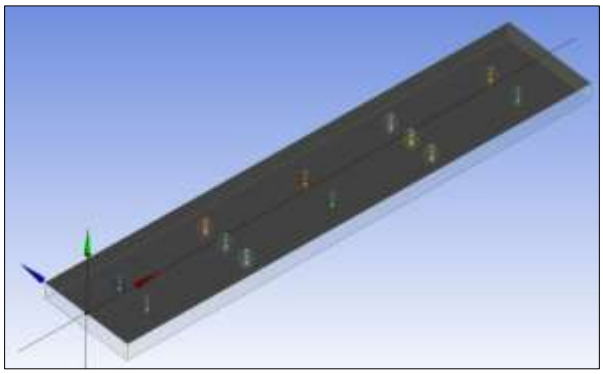

Figure 4b: Turbulators attached to the absorber plate inside the absorber duct

3. MESH CONFIGURATION

The model is meshed with 4.7 million elements with approximately the same number of elements for plain configuration and the turbulator configurations. Figure 5 shows the localized views of the meshed domain of the turbulator and the absorber duct.

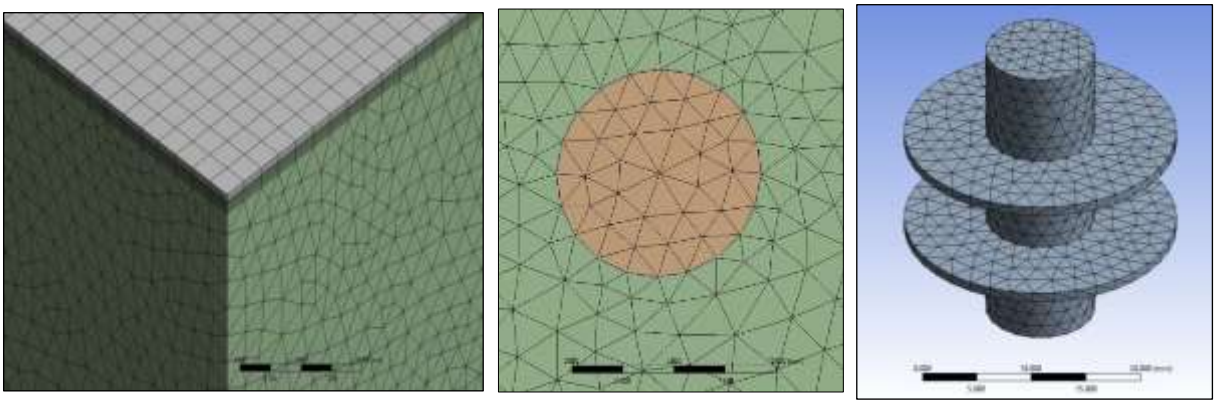

(a) (b) (c))

Figure 5 a) localized view of the meshed domain of absorber duct with boundary layer mesh, b) Localized plan view of the turbulator with fluid domain, c) meshed turbulator separated from the fluid domain

The grid independence check is carried out to decide the number of elements for the mesh size so as to get a grid independent result. It was found that the mesh size of 4.7 million elements and above gave variation which was less than 0.3% change in the output parameters and hence this grid size was adopted.

4. NUMERICAL SIMULATION

The CFD simulations are conducted using steady state condition available in the Ansys Fluent code. The governing equations, for momentum and mass are solved for the steady state flows. The SIMPLE algorithm of Patankar [11] is used to couple pressure and velocity. The Discretization is done using the first order and second order upwind schemes.

Mean flow equations in cartesian tensor notation are as givne in equations 1,2 and 3

Equation of continuity

$$\frac{\partial}{\partial x_i}(\rho U_i) = 0 \qquad (1)$$

Equation of momentum:

$$\frac{\partial}{\partial x_j}(\rho U_i U_j) = \frac{\partial P}{\partial x_i} + \frac{\partial}{\partial x_j}\left[\mu\left(\frac{\partial U_i}{\partial x_j} + \frac{\partial U_j}{\partial x_i}\right) - \rho\overline{u_i u_j}\right] \qquad (2)$$

Equation of energy:

$$\frac{\partial}{\partial x_j}(\rho U_i T) = \frac{\partial}{\partial x_j}\left[\frac{\mu}{\Pr}\frac{\partial T}{\partial x_j} - \rho\overline{u_i t}\right] \qquad (3)$$

For the 3D computational flow field, conservation equations are solved for the control volume to yield the pressure, temperature and velocity fields for the air flow in the duct and the temperature fields for the absorber plate. Convergence is reached when the residuals dropped below 1×10^{-6} in the computational domain.

The turbulence is affected by using $k-\varepsilon$ model with a turbulent intensity of 5%. The inlet condition specified is the mass flow rate corresponding to the Reynolds number. The outflow condition is applied at the outlet so as to account for the fully developed flow condition at the exit. Heat flux of 900 W is applied on the absorber plate to simulate the solar radiation heat as obtained from experimental study. No slip condition is applied on the walls and the thrmo physical properties of the absorber plate material are assume to remain constant with temperature.

5. VALIDATION OF THE PLAIN CONFIGURATION

The validation of the numerical results of plain duct configuration is carried out using Dittus Boelter equation as given in eq (4)

$$Nu = 0.023 * Re^{0.8} * Pr^{0.4} \qquad (4)$$

Table 1 shows the various parameters corresponding to Reynold's number from 3000 to 20000 along with validation results in terms of Nusselt number.

Table 1 Nusselt number validation for CFD analysis with Dittus Bolter equation

Re	$\dot{m}$ (kg/s)	Pr	Nu eq(4)	Nu CFD	% Change
3,000	0.00654	0.70115	12.07	10.41	13.76
10,000	0.021799	0.70094	31.62	27.92	11.72
20,000	0.043599	0.70089	49.3	46.60	5.4

It can be seen from table 1 that there is a reasonable agreement between the Nusselt number of CFD and empirical formula as given by the Dittus Bolter equation (4). It is also observed that the difference between the two values decreases with increase in Reynold's number.

6. RESULTS AND DISCUSSION

Turbulators of cylindrical shape with ribs are meant to act like fins with large surface area exposed to convective conditions inside the absorber duct. The radiation heat that is incident on the top surface of the absorber plate conducts and convects to the air flowing inside the absorber duct so as to heat the absorber air. The shape of the cylindrical turbulator with ribs tend to cause turbulence with minimum pressure loss across the duct as there are no sharp corners along the flow path. These turbulators also help in breaking the laminar sub layer that exists in the smooth duct which prevents heat transfer from taking place. The turbulators are provided at a pitch of 200 mm (pitch ratio $r_p = 1$) with alternatively two and three numbers of the same placed at the given pitch so as to allow smooth flow of the absorber air.

The thermal performances of the configuration with turbulators are quantified in terms of Nusselt number, convective heat transfer coefficient and the amount of pressure drop across the duct. They are compared with that of the smooth or plain duct configuration. Figure 6 shows the convective heat transfer coefficient of the two configurations for varying mass flow rate with Reynold's number ranging from 3000 to 20000. It can be seen from this figure that the convective heat transfer coefficient is having a large improvement over the plain duct configuration at the medium mass flow rate of Reynolds number 10000. It is also discernable that the convective heat transfer is higher than that of the plain configuration for the range of Reynolds number from 3000 to 20000. A similar trend is noticed from figure 7 where the Nusselt number is higher for all the mass flow rates for the turbulator configuration compared to that of the plain configuration. The improvement in Nusselt number is highest for the medium mass flow rate of Reynolds number 10000. However, it can be seen from figure 8 that the pressure drop across the duct increases significantly with increase in Reynolds number compared to that of the plain duct configuration. Figure 9 shows the plot of average absorber plate temperature coefficient $C_{AT} = (T_A - T_a)/T_a$ for the two configurations. It can be noted from this figure that the absorber plate temperature coefficient decreases with increase in mass flow rate and the absorber plate temperature of the turbulator configuration is lower than that of the plain configuration. This is indicative of the fact that turbulators are absorbing more heat from the absorber plate and transferring the heat to the absorber air. Figure 10 shows the temperature contour plot for configuration with turbulators. It is observed from this figure that the location where the turbulators are attached to the absorber plate, there is a significant decrease in the temperature. Also, the temperature drop across the plate is large near the upstream end of the duct as the temperature gradients are large towards the upstream. As the absorber air gains temperature while it moves towards the downstream there exists less temperature gradients between the absorber plate and the absorber air.

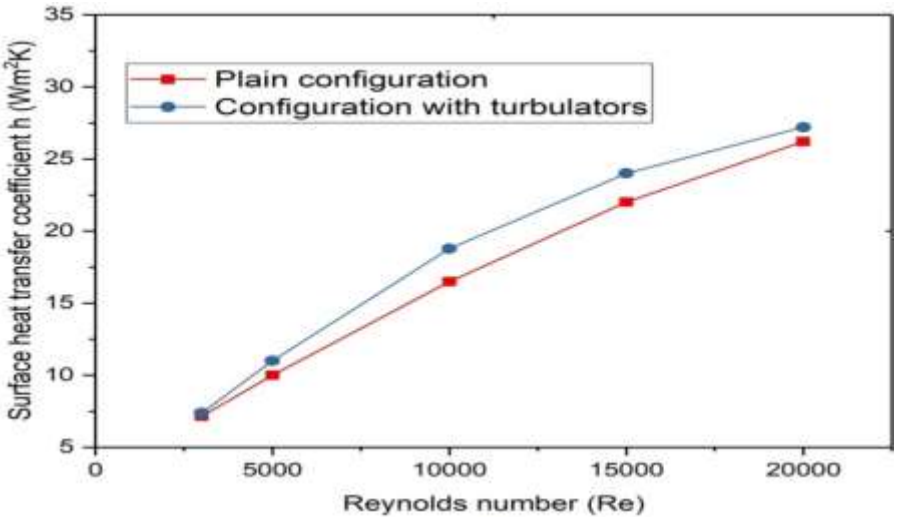

Figure 6 Variation of heat transfer coefficient with Reynolds number for configuration with turbulators and plain duct

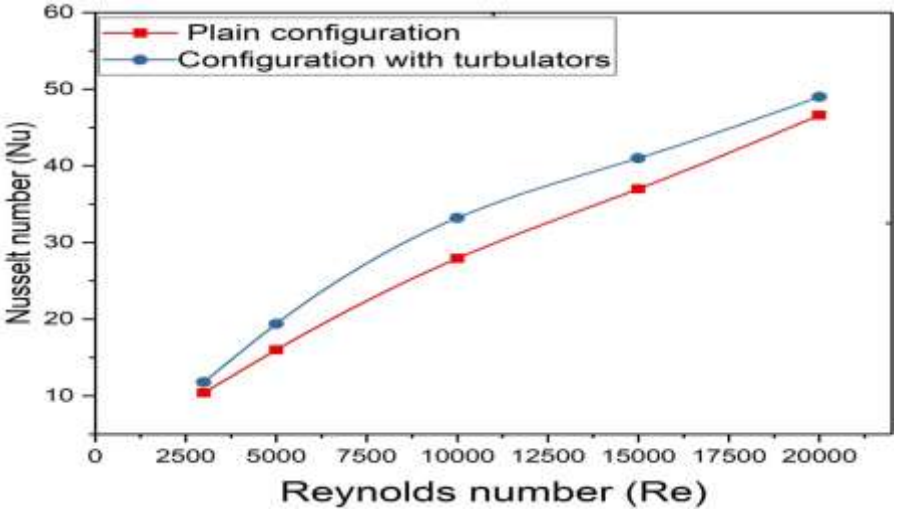

Figure 7 Variation of Nusselt number with Reynolds number for configuration with turbulators and plain duct

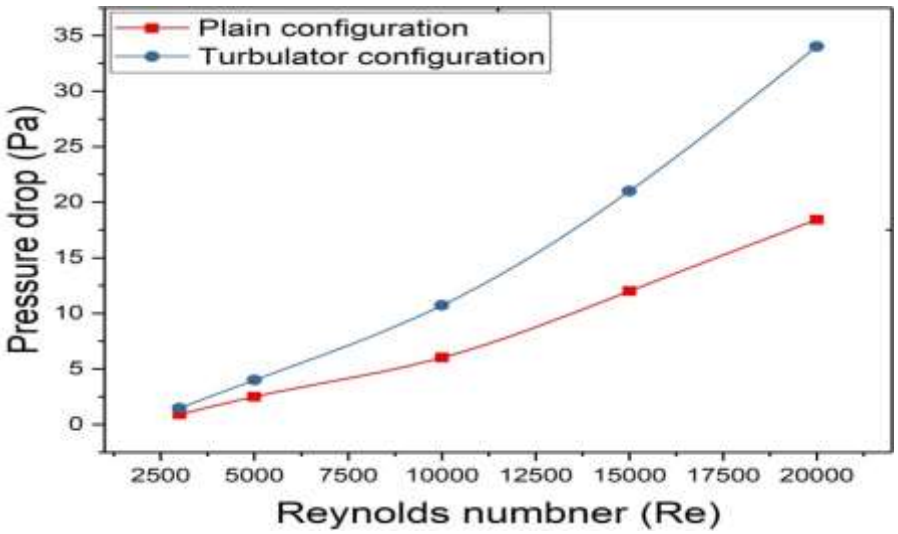

Figure 8 Pressure drop across the duct for configurations with and without turbulators

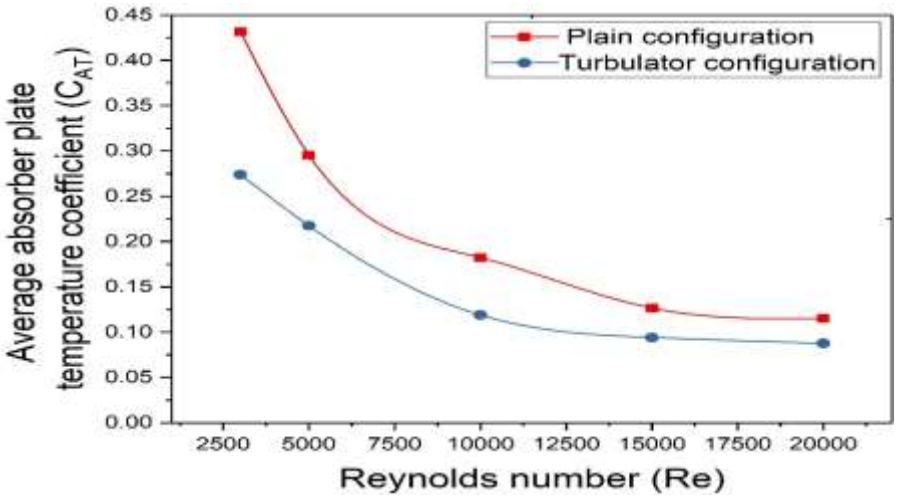

Figure 9 Plot of absorber plate temperature coefficient versus Reynolds number

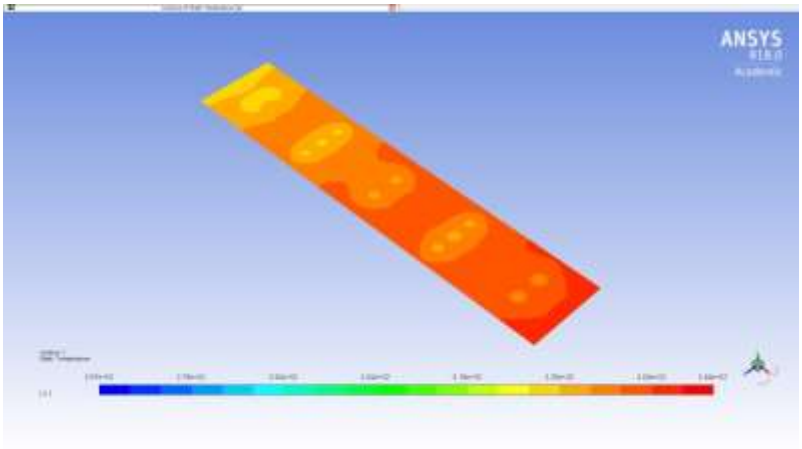

Figure 10 The absorber plate temperature plot for configuration with turbulators

The mechanism of convective heat transfer can be analyzed using figures 11 to 16 where the local temperature distributions are presented. This can be helpful for understanding the air heating process more precisely. Therefore, plain duct and the configuration with turbulators are compared to each other at a constant mass flow rate. Besides the same issue is shown from two different points of view. On the one hand Figure , 12 and 13 are displaying courses along x-direction at different duct heights and on the other hand Figure 14, 15 and 16 are showing the same across y-direction at different length positions. Both kinds of view are invers to each other.

The course drops at 300 mm and 700 mm in figures 11, 12 and 13 are caused by the turbulators themselves, because at these values the lines cross turbulators. Also at 100 mm, 500 mm and 900 mm the influence of the turbulators located next to the line is visible for the lines (y = 0 mm) placed at the lower absorber plate surface and (y = +0.5 mm) onto the plate's top. Otherwise it is visible that air near the heat transferring area (1 mm distance) is experiencing a large heating, but other air layers have only less heating. Same can be observed from figures 14, 15 and 16. Besides this it should be noted that enlarging the duct's height as large as possible is not recommendable. But it is also notable that the turbulators' helps in heating air layers which are far away (y < -15 mm) especially for Reynolds number of 20,000. Using turbulators it becomes easier to heat air more far away from heat transferring area.

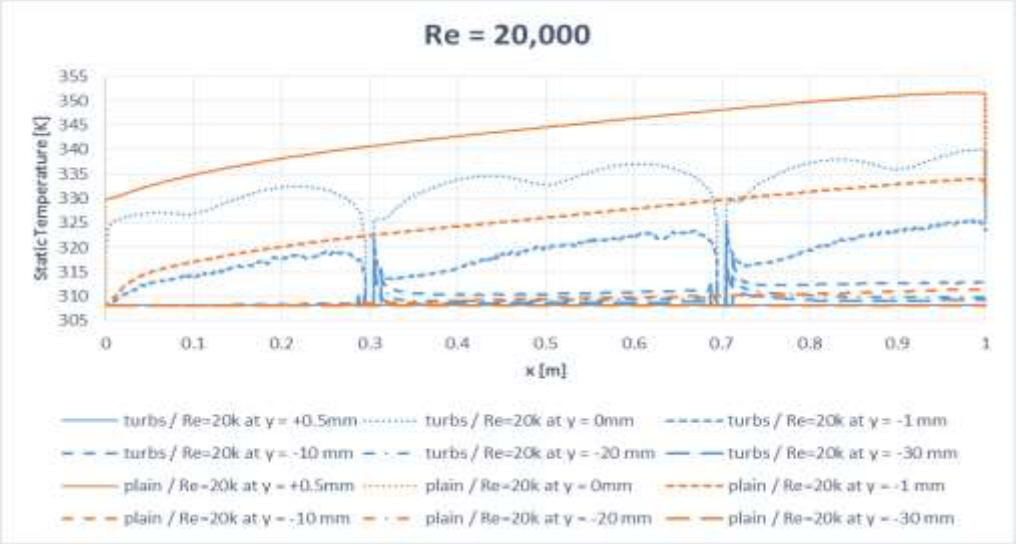

Figure 11 Local temperature across absorber duct at different heights for Re = 20,000

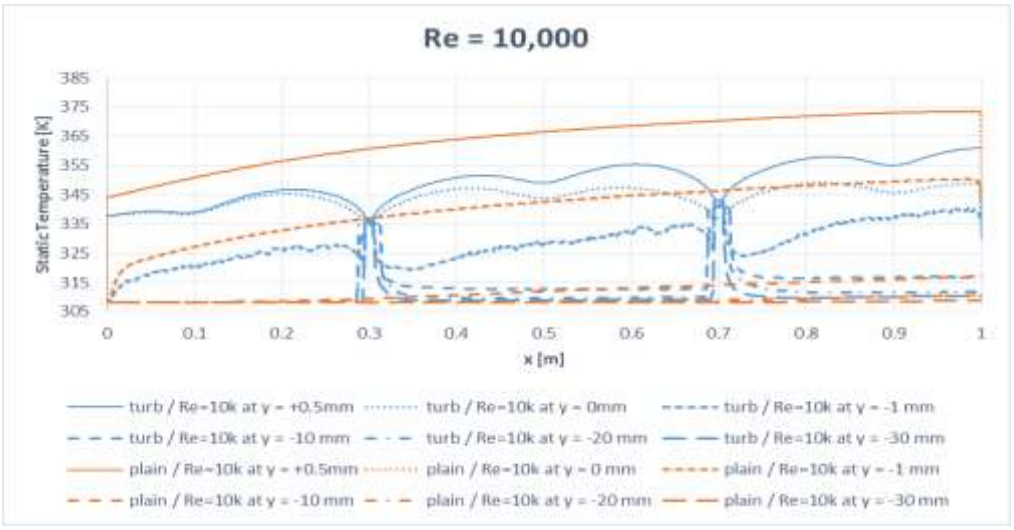

Figure 12 Local temperature across absorber duct at different heights for Re = 10,000

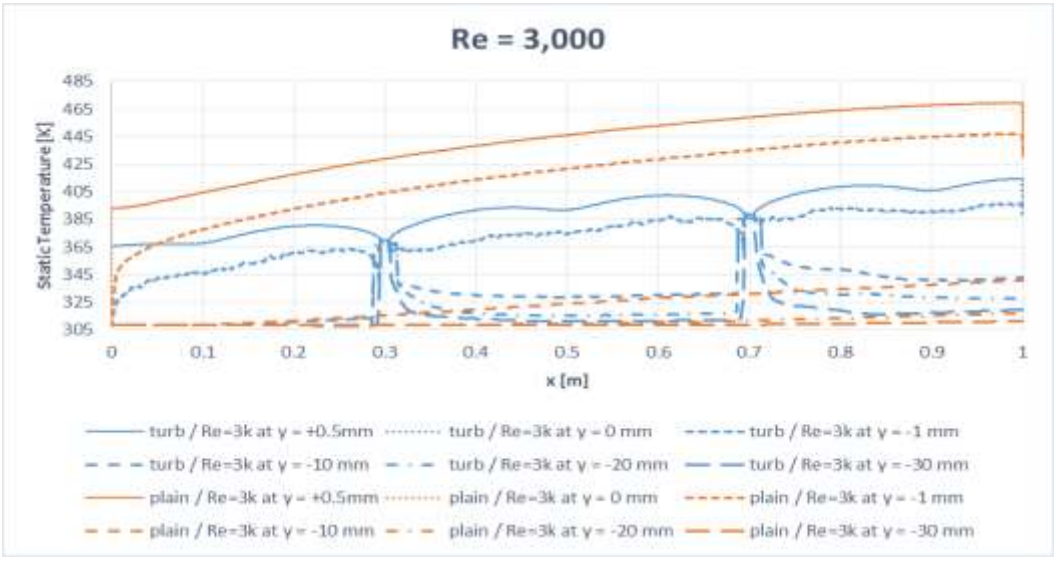

Figure 13 Local temperature across absorber duct at different heights for Re = 3,000

Figure 14 Local temperature across absorber duct height at different lengths for Re = 20,000

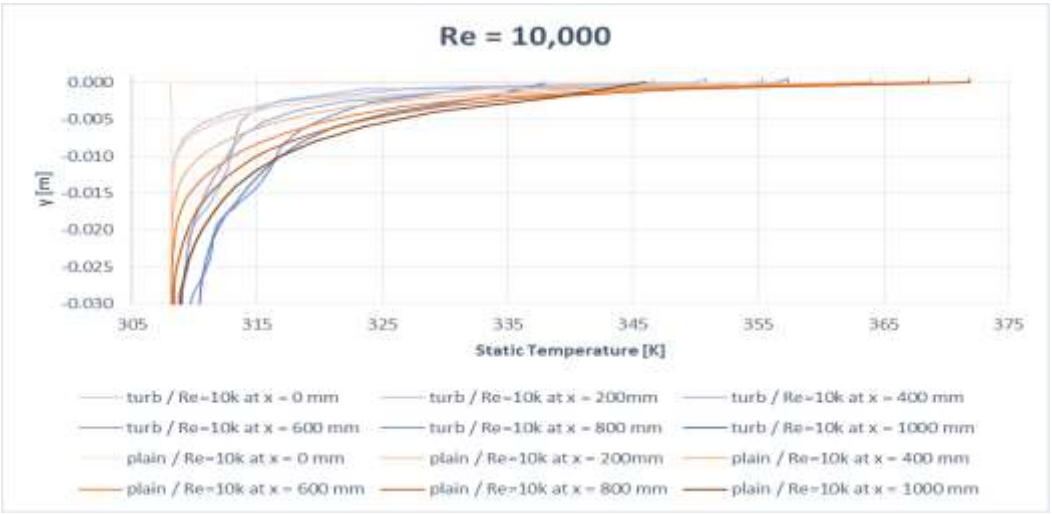

Figure 15 Local temperature across absorber duct height at different lengths for Re = 10,000

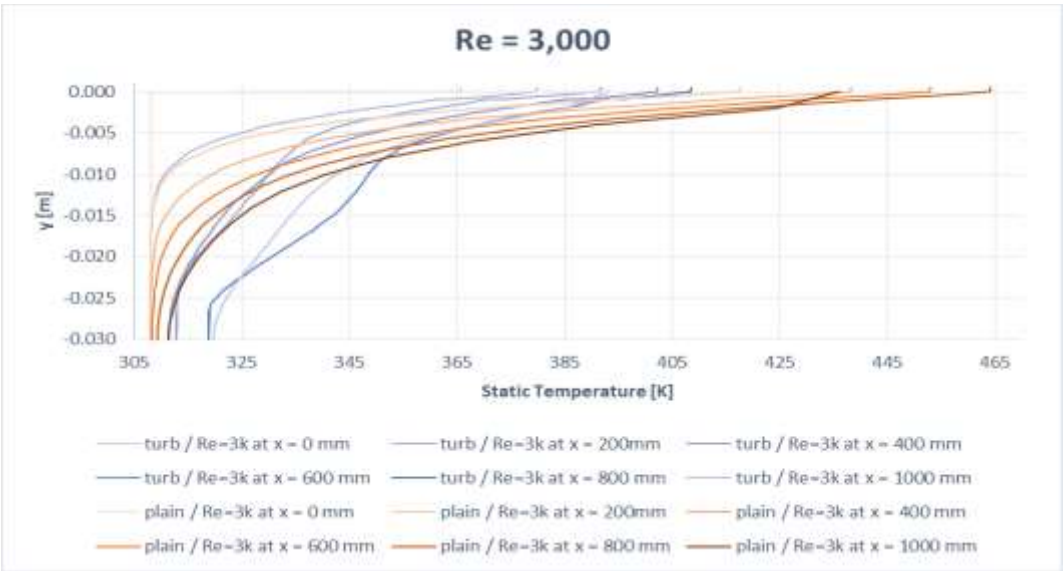

Figure 16 Local temperature across absorber duct height at different lengths for Re = 3,000

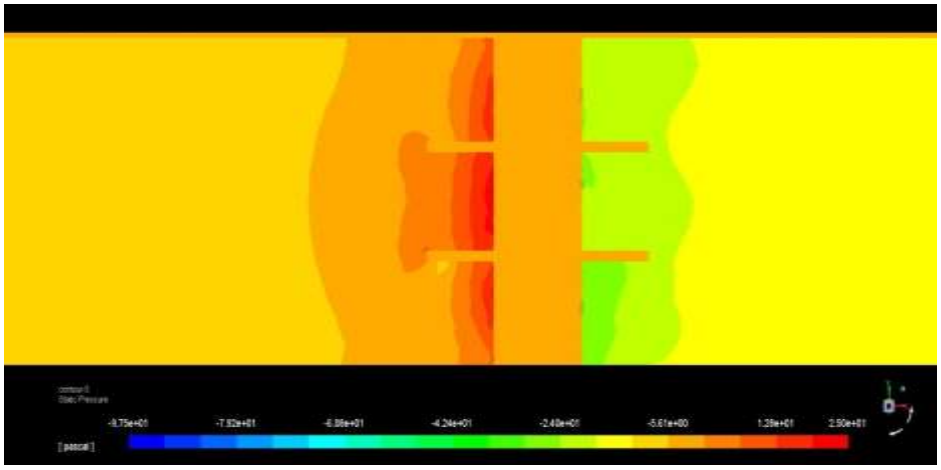

Figure 17 Pressure distribution plot across the turbulator

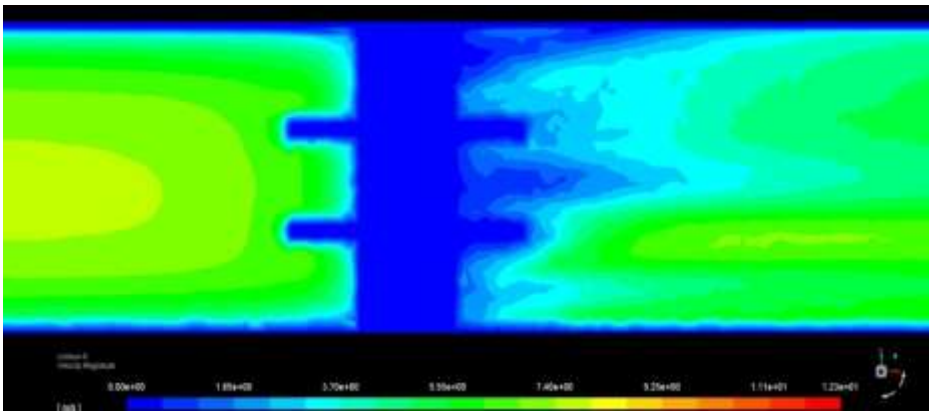

Figure 18 Velocity distribution across the turbulator

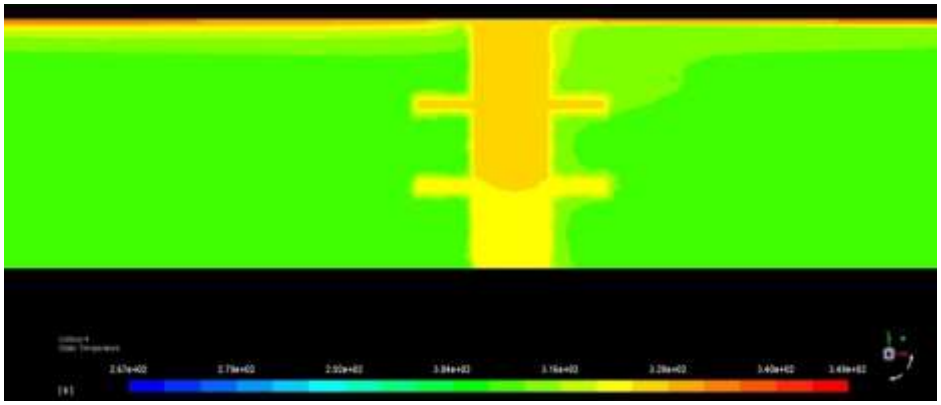

Figure 19 Temperature distribution across the turbulator

Figures 17 shows the pressure contour plots across a single turbulator. It is significant to note that the pressure rise is large near the eastern end of the turbulator between the ribs and the pressure drop is significant on the western end of the turbulator which leads to large turbulent region near the ribs as shown in the velocity contour plot of figure 18. The temperature contour plot shown in figure 19 indicates that the turbulator helps in imparting large amount of heat to the flowing fluid from the absorber plate to almost 2/3rd height of the turbulator.

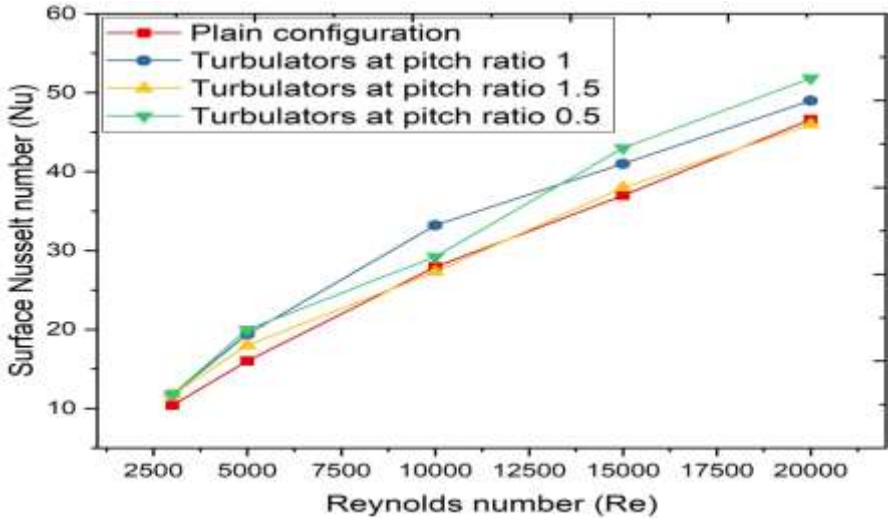

Figure 20 Nusselt number variation across the range of Reynolds number for varying pitch conditions

The analysis is further carried out for varying pitch conditions with pitch ratio varying from 0.5 to 1.5 with an increment of 0.5. The thermal performance in terms of Nusselt number and heat transfer coefficient are as shown in figures 20 and 21. It is significant to note that Nusselt number is seen to be significantly large for an axial pitch ratio of 1 when the Reynolds number is in the vicinity of 10000 whereas when the Reynolds number of the flowing air is increased to 20000, the configuration with a pitch ratio of 0.5 shows a significant improvement in the Nusselt number. The same trend is observed for the heat transfer coefficient as shown in fig 21. This could be attributed to the fact that when the pitch ratio is 1, the flow of fluid particle through the duct attains an optimal flow turbulence that enhances heat transfer capability of the air whereas at higher Reynolds number of 20000 the mass flow rate is sufficiently large enough to overcome the large array of turbulators of pitch ratio 0.5 which causes turbulence that enhances heat transfer. Figure 22 shows the plot of absorber plate temperature coefficient C_{AT} for varying mass flow rates with pitch ratio varying from 0.5 to 1.5. It is interesting to note from these plots that the absorber plate temperature decreases with decrease in pitch for the given range of mass flow rate. This is due to the reason that the absorber plate temperature drops with more number of turbulators attached to the absorber plate as the pitch.

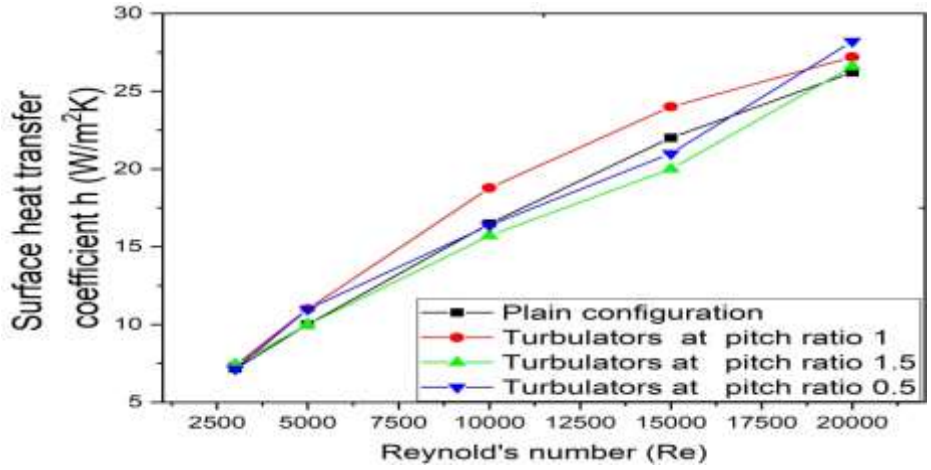

Figure 21 Heat transfer coefficient variation across the range of Reynolds number for varying pitch condition

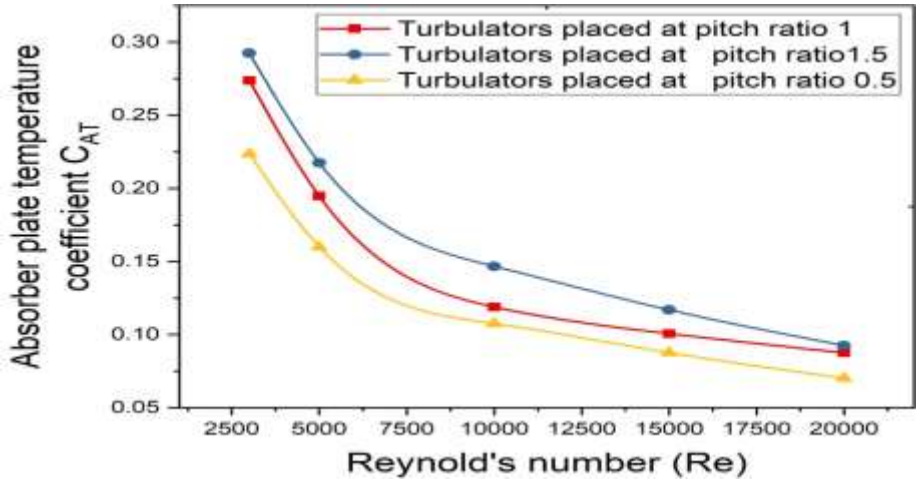

Figure 22 Average absorber plate temperature coefficient versus Reynolds number plot with varying pitch conditions

7. CONCLUSIONS

The numerical analysis of the solar air heater is carried out for a wide range of operating conditions and the following conclusions are drawn from the study.

- Cylindrical turbulators with ribs introduced inside the absorber duct of a solar air heater enhances the convective heat transfer capability for a wide range of mass flow rates.
- Turbulator configuration increases the Nusselt number of the collector by introducing turbulence throughout the absorber duct flow passage and thus enhances the thermal performance compared to that of the smooth duct configuration.
- Providing cylindrical turbulators with ribs tend to increase the pressure drop across the duct and thus demanding more pumping power to push the fluid against the turbulators at higher range of mass flow rate.
- Cylindrical turbulators with ribs tend to break the laminar sub layer near the absorber plate that exists in the smooth duct and causes the heat transfer to reach a greater depth of the fluid layer inside the absorber duct.
- Turbulators placed at a pitch ratio of 1 provides highest thermal performance of 18% in the neighborhood of flow Reynolds number 10000 and at a pitch ratio of 0.5, highest thermal performance of 12% is achieved at flow Reynolds number of 20000. Thus there exists an optimal performance corresponding to a given pitch ratio and Reynolds number.

NOMENCLATURE

Nu	Nusselt number
Re	Reynolds number
Pr	Prandtl number
k	thermal conductivity
ρ	Density
μ	Dynamic viscosity
U	Velocity
p	Pressure
T	Temperature

T_a Ambient temperature

T_A Absorber plate temperature

C_{AT} Absorber plate temperature coefficient

r_P Pitch ratio

ACKNOWLEDGMENT

Manipal Institute of Technology, Manipal Academy of Higher Education, Manipal provided the resources and facility for carrying out this research activity. This support is duly acknowledged by the authors.

REFERENCES

[1] Liu Ye-De, Diaz A, Suryanarayana N.V. (2009)" Heat Transfer Enhancement in Air-Heating Flat-Plate Solar Collectors". Journal Of Solar Energy Engineering.The American Society of Mechanical Engineers. Volume 106(3). DOI 10.1115/1.3267608.

[2] Persad P, Satcunanathan S. (2009)" The Thermal Performance of the Two-Pass, Two-Glass-Cover Solar Air Heater". Journal of Solar Energy Engineering .The American Society of Mechanical Engineers. Volume 105(3). DOI 10.1115/1.3266375.

[3] Giovanni Tanda, "Performance of solar air heater ducts with different types of ribs on the absorber plate", Energy, Volume 36, Issue 11, November 2011, pp. 6651–6660.

[4] Karwa Rajendra, Srivastava V.(2012)" Thermal Performance of Solar Air Heater Having Absorber Plate with V-Down Discrete Rib Roughness for Space-Heating Applications". Journal of Renewable Energy, Hindawi Publishing Corporation. Volume 2013, pp 1-13.

[5] Vasudeva K.Karanth, Manjunath M.S., N. Yagnesh Sharma, "Analysis of Solar Air Heater for [7] Enhancement of Thermal Performance Using Arc-Shaped Wire Turbulator".Fluid Engineering systems and Technologies, The American Society of Mechanical Engineers. Volume 7B, pp 1-8.

[6] Abhishek Saxenaa, , Varunb, A.A. El-Sebaiic, "A thermodynamic review of solar air heaters", Renewable and Sustainable Energy Reviews, Volume 43, March 2015, pp. 863–890.

[7] Kabeel A. E., A. Khalil, S. M. Shalaby and M. E. Zayed, "Investigation of the Thermal Performances of Flat, Finned, and v-Corrugated Plate Solar Air Heaters, J. Solar Energy Eng , ASME, 138(5), 051004 (Jul 19, 2016),PP 1 – 7.

[8] Satyender Singh and Prashant Dhiman, "Thermal Performance Analysis of a Rectangular Longitudinal Finned Solar Air Heater with Semicircular Absorber Plate", J. Solar Energy Engg ASME, 138(1), 011006 (Dec 08, 2015).

[9] M. S. Manjunath, K. Vasudeva Karanth, N. Yagnesh Sharma, "Numerical analysis of the influence of spherical turbulence generators on heat transfer enhancement of flat plate solar air heater", Energy 121 (2017), PP 616 – 630.

[10] M. S. Manjunath, K. Vasudeva Karanth, N. Yagnesh Sharma, "Numerical investigation on heat transfer enhancement of solar air heater using sinusoidal corrugations on absorber plate", International Journal of Mechanical Sciences, 138–139 (2018), PP. 219–228.

[11] Patankar, S.V., "Numerical heat transfer and fluid flow", 1st edition, Hemisphere Publishing Company., Minnesota USA, 1980.